

Application of a new microcantilever biosensor resonating at air-liquid interface for direct insulin detection and continuous monitoring of enzymatic reactions[†]

Jungwook Park,^{*a,b} Stanislav L. Karsten,^{a,c} Shuhei Nishida,^a Hideki Kawakatsu,^a and Hiroyuki Fujita^a

Received Xth XXXXXXXXXXXX 20XX, Accepted Xth XXXXXXXXXXXX 20XX

First published on the web Xth XXXXXXXXXXXX 200X

DOI: 10.1039/b000000x

Supplementary Materials

Theoretical model

The cantilever placed at the air-liquid interface significantly improved resolution of the biosensor. It has 50% higher quality factor and 5.7 times higher signal-to-noise ratio. A micro-slit around the cantilever separates the air and liquid phases at a meniscus. The meniscus membrane sustains liquid in the microchannel and works as spring to the resonance frequency. Park et al. described and modeled the spring constant for the surface tension at meniscus membrane as below¹.

The effect of surface tension is to resist against stretching of air-liquid: if the cantilever undergoes a tip deflection u , the area A increases, leading to an increase of the surface energy $W = \gamma A$, where γ is the surface tension of the liquid. It will be shown in the following that W can be written under the form:

$$W = W_{\text{constant}} + \frac{1}{2}ku^2 \quad (1)$$

The equation (2) means the membrane works as a spring. air-liquid can be approximated as depicted in Fig. 1, including the front trapezoidal shape $CDEF$, two times the triangle BCD and two times the lateral area $OACB$.

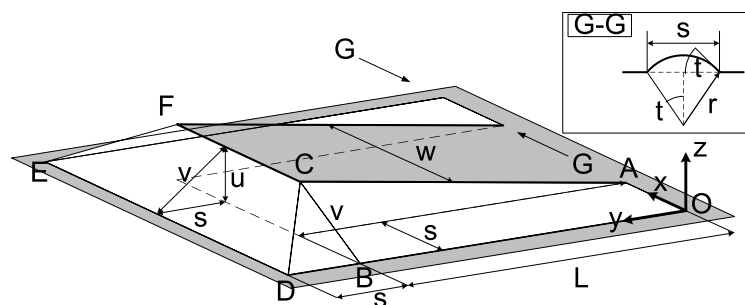


Fig. 1 Sketch of the cantilever (length L and width w), a slit of width s and a gas-liquid interface, made of a trapezoidal shape $CDEF$, two triangles BCD and two lateral areas $OACB$. The cantilever tip deflection, u , is assumed to be smaller than s and L . G-G: sketch of a deformed air-liquid interface along the slit: one of the curvatures is equal to zero, while the second one is equal to $1/r$.

The geometry depicted in Fig. 1 is only an approximation, for two reasons: (1) the cantilever does not bend linearly; (2) the air-liquid interface must respect the so-called Laplace equation, *i.e.* present a constant curvature if the pressure is assumed to be constant in the liquid side of the interface. Obviously, this condition is not respected by the proposed geometrical shapes (1 trapeze + 2 triangles + 2 lateral areas), but the proposed model can at least determine the order of magnitude of the effect of surface tension². Let us now compute the area of the three geometries, with the assumption that $u \ll s \ll L$:

1. Trapezoidal shape $CDEF$:

$$\begin{aligned} A_I &= \frac{(\|ED\| + \|CF\|)v}{2} \\ &= (w+s)s\sqrt{1 + \left(\frac{u}{s}\right)^2} \\ &\approx (w+s)s\left(1 + \frac{1}{2}\frac{u^2}{s^2}\right) \end{aligned} \quad (2)$$

2. Two times the triangular shape BCD :

$$\begin{aligned} A_{II} &= 2\frac{\|DB\| \cdot \|BC\|}{2} \\ &= s \cdot v \\ &\approx s^2\left(1 + \frac{1}{2}\frac{u^2}{s^2}\right) \end{aligned} \quad (3)$$

3. Two times the lateral area $OACB$ shown in Fig. 1:

The z -coordinate of P' is equal to $z(P') = u\frac{x}{s}$, leading to the z -coordinate of an arbitrary point P :

$$z(P) = xy\frac{u}{sL} = xyQ \quad (4)$$

with $Q = \frac{u}{sL}$.

Now, the surface element of the lateral area $OACB$ can be expressed as:

$$\begin{aligned} dS &= \sqrt{1 + \left(\frac{\partial z}{\partial x}\right)^2 + \left(\frac{\partial z}{\partial y}\right)^2} dx dy \\ &= \sqrt{1 + Q^2(x^2 + y^2)} dx dy \\ &\approx \left(1 + \frac{1}{2}Q^2x^2 + \frac{1}{2}Q^2y^2\right) dx dy \end{aligned} \quad (5)$$

and the area of both lateral interfaces can be written as:

$$A_{III} = 2 \int_0^s \int_0^L dS$$

$$\approx 2 \left[Ls + \frac{u^2}{6sL} (s^2 + L^2) \right] \quad (6)$$

Summing up $A = A_I + A_{II} + A_{III}$ and multiplying by surface tension γ to get the surface energy, we find:

$$W = \underbrace{\gamma(ws + 2s^2 + 2sL)}_{W_{\text{constant}}} + \frac{1}{2} u^2 \underbrace{\gamma \left(2 + \frac{w}{s} + \frac{2}{3} \frac{s^2 + L^2}{sL} \right)}_k \quad (7)$$

which means that the smaller-width slit has a larger spring constant caused by the surface tension. According to analysis, the width of the micro-slit (s) and the surface tension coefficient (γ) change the elastic property of the meniscus membrane. Then, the spring constant on the meniscus membrane at the micro-slit can be expressed by the equation as below.

$$k_{\Delta\gamma} = \gamma \left(2 + \frac{w}{s} + \frac{2}{3} \frac{s^2 + L^2}{sL} \right) \quad (8)$$

Then, the resonance frequency of the cantilever with additional mass (ΔM_b) and surface tension changes ($k_{\Delta\gamma}$) is given by the following formula using a concentrated mass and a spring model.

$$f_R + \Delta f_R = \frac{1}{2\pi} \sqrt{\frac{k_{Si} + k_{\Delta\gamma}}{M_{Si} + \Delta M_b}} \quad (9)$$

f_0 : initial resonance frequency, Δf_R : additional resonance frequency, k_{Si} : Spring constant of silicon cantilever ($Ewt^3/4L^3$), $k_{\Delta\gamma}$: Spring constant of meniscus membrane (Surface tension, described above), L : length of cantilever ($l = 80\mu\text{m}$, $w = 20\mu\text{m}$, and $t = 5\mu\text{m}$), E : Young's modulus ($169 \times 10^9 \text{ N/m}^2$), M_{Si} : mass of cantilever ($18.64 \times 10^{-9} \text{ g}$), and ΔM_b : additional mass

Table 1 shows the estimated resonance frequency shift by the loaded mass of biomolecules (insulin). The loaded mass (ΔM_b) can be calculated by binding density (ρ) x area of surface ($l \times w$), ($\rho_b = 3.8 \times 10^{-9} \text{ mole/m}^2$, molecular weight of insulin: 5.808 kDa). Theoretical density of APTES ($\rho_{\text{calculation}}$) on

Table 1 Weight of antibodies, insulin, and the resonance frequency shift by them

Items	Anti-insulin antibody		Insulin	
	by ΔM_b	by $k_{\delta\gamma}$	by ΔM_b	by $k_{\delta\gamma}$
Molecular weight (g)	2.5×10^{-19}		9×10^{-21}	
Molecular weight (kDa)	150		5.8	
Added mass on cantilever surface ($\rho_b \times l \times w$)	$9.1 \times 10^{-13} \text{ g}$		$7.1 \times 10^{-14} \text{ g}$	
Surface tension (mN/m)		71		61
Δf_R (kHz)	19.1	0.02	1.53	0.12

SiO_2 surface is $130 \times 10^{-9} \text{ mole}/\text{m}^2$, when APTES is deposited on the substrate homogeneously. However, the binding density (ρ_b) of biomolecules is varied depending on the size of molecules. Rajendra R Bhat et. al has reported the binding density of 17 nm-gold-bead peptide-bonded on the APTES-coated substrate. The maximum binding density is $0.83 \times 10^{-9} \text{ mole}/\text{m}^2$ in optimized condition⁷. According to the calculation, we can estimate the binding density for antibodies of $3.8 \times 10^{-9} \text{ mole}/\text{m}^2$ on a substrate because the size of antibodies is 7.8 nm^3 .

The mass of insulin antibody is about 150 kDa ($2.5 \times 10^{-19} \text{ g}$) and we estimate the resonance frequency shift of 19.1 kHz by the mass of antibodies ($9.1 \times 10^{-13} \text{ g}$) deposited on the cantilever. And the resonance frequency shift by captured insulin is calculated to be 1.53 kHz (Δf_R). Furthermore, the resonance shift by the surface tension changes can be negligible.

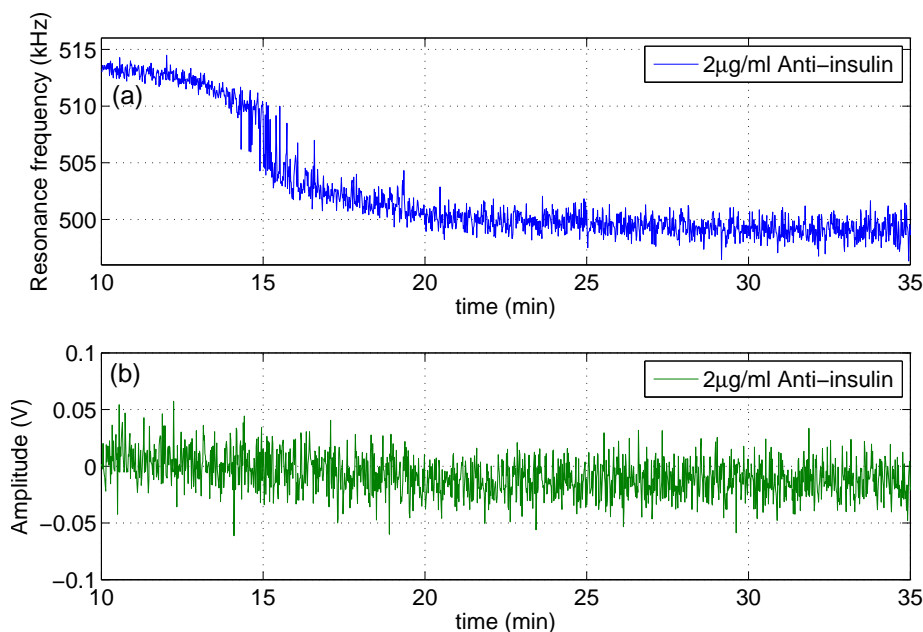


Fig. 2 Resonance frequency (a) and amplitude (b) response of cantilever by anti-insulin antibody binding.

Viscoelastic response

When a cantilever vibrates at the resonance condition, the changes in the viscoelastic characteristics mainly influence the amplitude and the quality factor. While measuring the f_R of the cantilever we measure the amplitude shift simultaneously as shown in figures. The amplitude decreased after the sample injection. The decrease in the amplitude is mainly attributed to the change in the hydrodynamic drag, which is caused by the adsorption of biological molecules (Fig. 2).

An advantage of our cantilever sensor is that the efficiency of photothermal excitation is not affected by the surface change, for example the reflectivity change caused by the adsorption of the biological molecules. Thus, our setup would be applicable for measuring time-dependent transition in the dynamic mechanical

property of the cantilever sensor.

References

- 1 J. Park, S. Nishida, P. Lambert, H. Kawakatsu and H. Fujita, *Lab on a chip*, 2011, **11**, 4187–4193.
- 2 P. Lambert, M. Mastrangeli, J. B. Valsamis and G. Degrez, *Microfluid and Nanofluid*, 2010, **9**, 797–807.
- 3 N. Ban, C. Escobar, R. Garcia, K. Hasel, J. Day, A. Greenwood and A. Mcpherson, *Proc. Natil. Acad. Sci.*, 1994, **91**, 1604–1608.

† Electronic Supplementary Information (ESI) available: [details of any supplementary information available should be included here]. See DOI: 10.1039/b000000x/

^a Center for International Research on Micronano Mechatronics (CIRMM), Institute of Industrial Science (IIS), the University of Tokyo, 4-6-1 Komaba Meguro, Tokyo, 153-8505, Japan. Fax: +81 3 5452 6250; Tel: +81 3 5452 6248

^b Current address: California Institute of Technology, 1200 E. California Blvd MC 136-93, Pasadena, California, USA; E-mail: jwpark@caltech.edu

^c NeuroInDx, Inc., Signal Hill, California, USA; E-mail: skarsten@neuroindx.com

‡ Additional footnotes to the title and authors can be included e.g. 'Present address:' or 'These authors contributed equally to this work' as above using the symbols: ‡, §, and ¶. Please place the appropriate symbol next to the author's name and include a \footnotetext entry in the the correct place in the list.